Reflection-based Relaying Techniques in Visible Light Communications: Will It Work?

BORJA GENOVÉS GUZMÁN[1]**, (Student Member, IEEE), CHENG CHEN**[2]**, (Member, IEEE), VÍCTOR P. GIL JIMÉNEZ**[3]**, (Senior Member, IEEE), HARALD HAAS**[2]**, (Fellow, IEEE), AND LAJOS HANZO**[4]**, (Fellow, IEEE)**
[1]IMDEA Networks Institute, 28918 Leganés (Madrid), Spain (e-mail: borja.genoves@imdea.org)
[2]Institute for Digital Communications, Li-Fi R&D Centre, School of Engineering, The University of Edinburgh, EH8 9YL Edinburgh, U.K. (e-mail: cheng.chen@ed.ac.uk; h.haas@ed.ac.uk)
[3]Department of Signal Theory and Communications, University Carlos III of Madrid, 28911 Leganés (Madrid), Spain (e-mail: vgil@tsc.uc3m.es)
[4]School of Electronics and Computer Science, University of Southampton, SO17 1BJ Southampton, U.K. (e-mail: lh@ecs.soton.ac.uk)

Corresponding author: Lajos Hanzo (e-mail: lh@ecs.soton.ac.uk).

ABSTRACT Visible light communication (VLC) is capable of satisfying the escalating data rate demand in indoor scenarios. The lighting infrastructure may also be exploited in the downlink of a wireless local area network (WLAN), where light-emitting diodes are used for transmitting information. The backhaul of VLC access points (APs) constitutes a potential bottleneck in WLANs, especially in large rooms where the number of APs is high. Thus, an alternative reflection-based cooperative wireless system concept is proposed, where no wired connections are required for connecting the APs. Then, its data rate analysis is developed based on the signal-to-noise ratio attained. The results show that the performance of the cooperative wireless system advocated closely approximates the performance of the traditional wired backhaul. Finally, we demonstrate by using Jain's index of fairness that the proposed scheme provides fair coverage quality for all users.

INDEX TERMS Cooperative transmission, joint transmission, relaying techniques, visible light communication.

I. INTRODUCTION

THERE is an ever-increasing demand for wireless data services that ultimately requires new spectrum beyond the radio-frequency (RF) [1] band. Visible light communication (VLC) is a promising technique capable of simultaneously providing both high data rates and illumination. Since VLC uses optical wavelengths, it does not interfere with RF systems and its propagation can be controlled, whilst additionally improving the physical layer security. RF and VLC systems can work together and complement each other [2], creating a heterogeneous network, as considered in the new mobile communication standards [3] [4].

VLC typically uses intensity modulation/direct detection (IM/DD), which means that the signals have to be real-valued and unipolar. Light-emitting diodes (LEDs) act as transmitters, whereas photodiodes (PDs), which operate as receivers, directly collect the optical power and convert it into an electrical signal. Orthogonal frequency division multiplexing (OFDM) schemes have found their way into numerous standards and have also been adapted to optical signals, leading to optical-OFDM (O-OFDM) schemes [5].

VLC has mainly been studied in indoor scenarios, albeit there is also an outdoor solution in the open literature [6]. The light-fidelity (LiFi) concept was coined by Haas [7] and refers to a fully networked VLC system, where light fixtures are interconnected for providing Internet access to all users in a room. Each light fixture serves as an access point (AP) that creates a small-cell network known as an attocell network [8], which is reminiscent of the femtocell concept [9]. However, the use of small cells tends to impose increased inter-cell interference (ICI) in regions where more than one AP provides coverage. Besides, VLC suffers from line-of-sight (LoS) link blockage events between the LED and the PD. Several techniques have been proposed for mitigating

IEEE Access

B. Genovés Guzmán *et al.*: Reflection-based Relaying Techniques in Visible Light Communications: Will It Work?

ICI in attocell networks and for providing coverage from more than one AP in order to make LiFi realizable. Cheng *et al.* [8] proposed joint transmission techniques for improving the throughput, while fractional frequency reuse techniques [10] were invoked for striking a compromise between the cell-edge performance and the system throughput. As a further development, space division multiple access (SDMA) techniques were proposed for attocell networks in [11]. The application of multiple-input multiple-output (MIMO) VLC solutions was advocated for example by Zeng *et al.* [12] and Azhar *et al.* [13]. Furthermore, some studies of cooperative techniques have already been carried out for overcoming the LoS-link blockage using on-off keying (OOK) and direct current-biased optical OFDM (DCO-OFDM) in [14] and [15], respectively.

However, all these techniques rely on a wired backhaul that is often assumed to be ideal [16], i.e. lossless, noiseless as well as instantaneous, which theoretically assumes having unlimited capacity. Naturally, this is an unrealistic scenario. A backhaul link is essential in cellular networks [17] either for connecting base stations (BSs) as in Long Term Evolution (LTE) [18], or for linking BSs with a central controller that manages the traffic as in the Global System for Mobile communications (GSM) standard [19]. Thus, the study of a backhaul link is crucial for realistically evaluating the overall performance. A variety of wired backhaul techniques have been proposed for VLC. For example, Song *et al.* [20] implemented indoor broadband broadcast systems based on a sophisticated combination of VLC and power line communication (PLC), where they used the power line network as the backbone. Ethernet-based VLC can also be employed for providing connectivity to the fixtures, as Delgado *et al.* demonstrated in [21]. Naturally, optical fiber may also serve as the backbone [22].

However, the use of wired backhaul imposes an extra cost and cabling infrastructure, resulting in an increased complexity, especially when the network becomes larger, i.e., when cell densification and cooperation is required. It has been richly documented in [23] that a wired backhaul deployment complicates the deployment of a LiFi network, although, naturally, it would indeed improve the quality of backhaul communication. Thus, practical wireless backhaul links have been studied using RF systems [24] or free-space optical (FSO) communications [25]. The installation of a LiFi system in a room can be even more costly, if significant alterations to the room are necessary to equip the light fixtures with LiFi capabilities. To this end, the first treatise on the viability of a wireless backhaul in LiFi systems was published in [23]. Furthermore, relay-assisted techniques were considered as suitable alternatives to support the main link and improve the system throughput. In this context, Narmanlioglu *et al.* [26] presented a cooperative VLC system using an intermediate light source that acts as a relay terminal. Na *et al.* proposed [27] a relaying technique using an asymmetrically clipped direct current biased optical OFDM (ADO-OFDM) scheme to relay information and to transmit
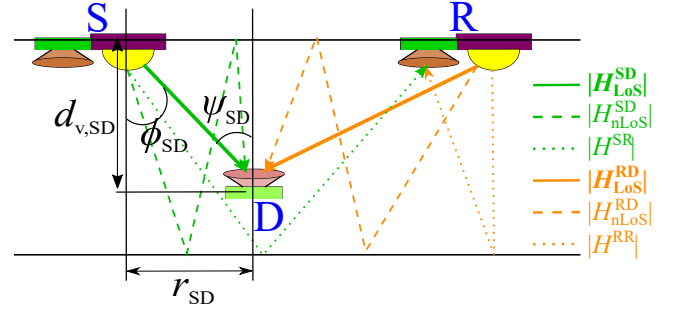

FIGURE 1. Reflection-based relaying scenario.

its own data using odd and even subcarriers, respectively. Furthermore, Kizilirmak *et al.* [28] investigated the bit error ratio (BER) performance of a relay-assisted VLC system, where the main light source on the ceiling and an additional desk light are used.

In contrast to the existing studies, this paper proposes a cooperative VLC system based on relay-assisted techniques, where the signal-reflections gleaned are beneficially exploited as relaying links. Relaying techniques were utilized in [23], but 6 extra LEDs in addition to several PDs were needed in order to build a mesh network. In our solution only a single additional PD is needed per AP, which reduces the hardware complexity. This way, the knowledge of the neighboring APs location or network topology is no longer required, which would speed-up the deployment of a LiFi network. This relaying-based principle makes our LiFi proposal beneficial in the presence of blocking elements, which is a common indoor scenario, because the system performance remains satisfactory even in case of LoS blockage events.

This paper is organized as follows. Section II discusses the system model. Section III carries out a downlink study where signal-to-noise ratio (SNR) equations are derived for various relaying techniques. Then, SNR optimization is carried out in Section IV. Section V presents a realistic squared-lattice scenario and derives a performance bound. Finally, in Section VI we discuss the results obtained and in Section VII we offer our conclusions.

II. SYSTEM MODEL

Fig. 1 illustrates the reflection-based relaying technique proposed. The system supports one source S, one selected relay R and one destination (user) D. The source is the AP closest to the destination and the relay selected is the neighboring AP, which is closest to the user. The channels spanning from S and R to D are represented by $|H_{\text{LoS}}^{\text{SD}}|$ and $|H_{\text{LoS}}^{\text{RD}}|$, respectively, both with their corresponding non-line-of-sight (nLoS) paths denoted by $|H_{\text{nLoS}}^{\text{SD}}|$ and $|H_{\text{nLoS}}^{\text{RD}}|$ (see Fig. 1). Every AP is formed by one LED and one PD, both having a vertical downward orientation. The self-interference produced at R is represented by the $|H^{\text{RR}}|$ channel due to full-duplex transmission and reception [1]. The relay R takes advantage of the reflections produced by the floor $(|H^{\text{SR}}|)$ to receive the signal transmitted by the source S, to process it

IEEE Access®

B. Genovés Guzmán *et al.*: Reflection-based Relaying Techniques in Visible Light Communications: Will It Work?

a. Time-domain free-space channel impulse responses.

b. Magnitude of the free-space channel impulse responses in frequency-domain.
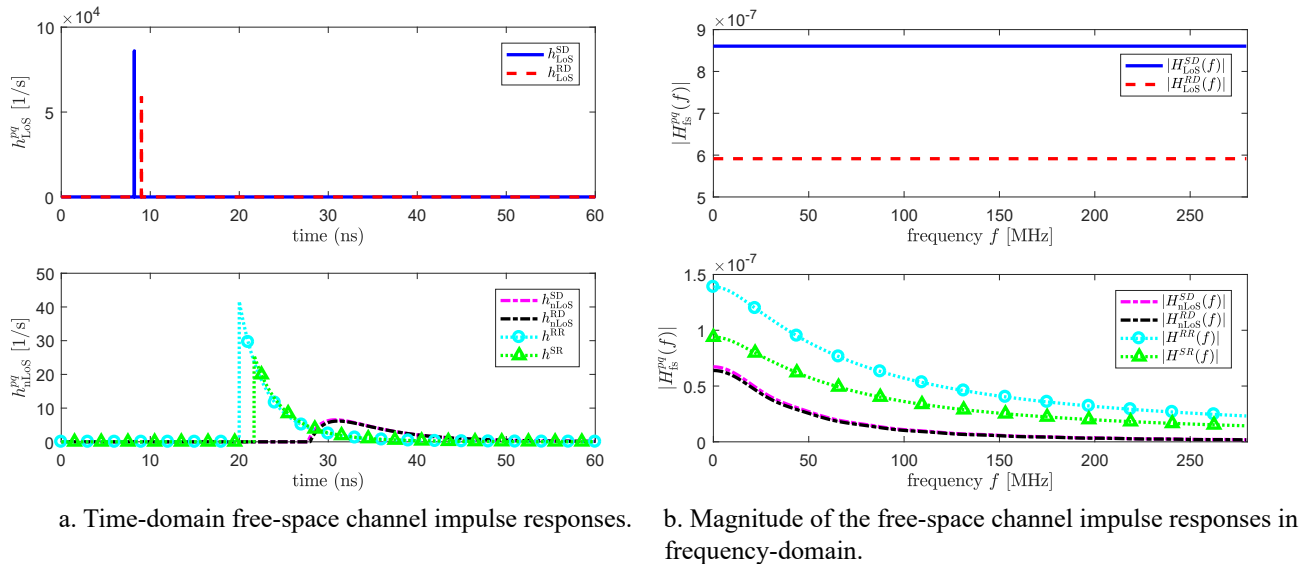
FIGURE 2. Illustration of the channel impulse responses in a simple scenario, where the coordinates of the source S, relay R and destination D are in meters [0.5; 2.5; 3], [3; 2.5; 3] and [1.5; 2.5; 0.75], respectively. Parameters: $\rho_{\text{floor}} = 0.6$, $\rho_{\text{ceil}} = 0.8$, $W = 280\,\text{MHz}$, $n_{\text{ref}} = 1.5$, $\psi_{\text{FoV}} = 90°$, $\phi_{1/2} = 60°$, $G_f = 1$, $A_r = 8.72\,\text{mm}^2$.

and forward it to the destination D. As a worst-case scenario, only reflections from the floor are considered, since not all the APs are located close to a wall. Nonetheless, reflections from the walls could readily be considered, which would make the relaying path stronger. Although numerous contributions assume that wall-reflections are negligible, they have been demonstrated to be dependent on the specific material, finish, color and shade of the surfaces [29] [30]. The field-of-view (FoV) at the receivers is assumed to be wide enough for allowing communication among the S, R and D. In that way, the loss caused by a LoS blockage at any link can be mitigated by exploiting this relaying principle.

A. CHANNEL MODEL

The channel model is essentially determined by the front-end devices (LED and PD) and the free-space transmission. The frequency domain channel transfer function (FDCHTF) between the LED p and PD q is formulated as

$$|H^{pq}[k]| = |H_{\text{fe}}[k]| \cdot |H_{\text{fs}}^{pq}[k]|, \tag{1}$$

where $|H_{\text{fe}}[k]|$ is the FDCHTF of the front-end devices in the k-th subcarrier modeled as defined in Eq. (1) of [31] or Eq. (8) and (9) of [32]

$$|H_{\text{fe}}[k]| = \sqrt{\exp\left(-\frac{kW}{KF_{\text{fe}}}\right)}, \tag{2}$$

where K is the number of frequency domain (FD) subcarriers spanning the total bandwidth W and F_{fe} is the so-called bandwidth factor that controls the FD characteristics. The free-space FDCHTF $|H_{\text{fs}}^{pq}[k]|$ between the AP p and q is derived from the channel impulse response (CIR) by the discrete Fourier transform as $|H_{\text{fs}}^{pq}[k]| =$

$\int_0^\infty h_{\text{fs}}^{pq}(t) e^{-\frac{2\pi j W t k}{K}} \, \mathrm{d}t$. The CIR is composed by the LoS and nLoS components as

$$h_{\text{fs}}^{pq}(t) = 1_{\text{block}}^{pq} h_{\text{LoS}}^{pq}(t) + h_{\text{nLoS}}^{pq}(t), \tag{3}$$

where 1_{block}^{pq} is 1 or 0, if either LoS or nLoS propagation occur, respectively. The LoS component is expressed as [32]

$$\begin{aligned} h_{\text{LoS}}^{pq}(t) &= \frac{(m+1)G_f G_c A_r}{2\pi \left(r_{pq}^2 + d_{\text{v},pq}^2\right)} \cos^m(\phi_{pq}) \cos(\psi_{pq}) 1(\psi_{pq}) \delta(t - \tau_{\text{LoS}}) \\ &= \frac{(m+1)G_f G_c A_r d_{\text{v},pq}^{m+1}}{2\pi \left(r_{pq}^2 + d_{\text{v},pq}^2\right)^{\frac{m+3}{2}}} 1(\psi_{pq}) \delta(t - \tau_{\text{LoS}}), \end{aligned} \tag{4}$$

where m is the Lambertian emission order defined as $m = \frac{-1}{\log_2 \cos(\phi_{1/2})}$, where $\phi_{1/2}$ is the half-power semi-angle of the LED. The optical filter's loss at the receiver is denoted by G_f and $G_c = n_{\text{ref}}^2 / \sin^2(\psi_{\text{FoV}})$ represents the concentrator gain, where n_{ref} is the refractive index of the material that composes the concentrator and ψ_{FoV} is the FoV at the receiver. The PD's physical area is denoted by A_r, while r_{pq} and $d_{\text{v},pq}$ are the horizontal and vertical distances between the transmitter p and the receiver q, respectively. The angle of irradiance between p and q is denoted by ϕ_{pq}, whereas the angle of incidence is ψ_{pq}. The delta function is denoted by $\delta(\cdot)$ and the propagation delay of light between p and q is determined by $\tau_{\text{LoS}} = \sqrt{r_{pq}^2 + d_{\text{v},pq}^2}/c$, where $c \approx 3 \cdot 10^8$ m/s is the speed of light in vacuum. Still referring to (4), the Boolean variable $1(\psi_{pq})$ indicates whether the LoS transmission is within the FoV of the receiver or not and it is defined as

$$1(\psi_{pq}) = \begin{cases} 1, & \text{if } \psi_{pq} \leq \psi_{\text{FoV}} \\ 0, & \text{if } \psi_{pq} > \psi_{\text{FoV}} \end{cases}. \tag{5}$$

The nLoS component of the CIR between p and q $h_{\text{nLoS}}^{pq}(t)$ seen in Fig. 1 may be formulated according to the analytical

IEEE Access

B. Genovés Guzmán *et al.*: Reflection-based Relaying Techniques in Visible Light Communications: Will It Work?

method presented in [29], which relies on the transmitter and user locations in the room, on their orientations, as well as on A_r, m, ψ_{FoV} and the reflectances of the surfaces ρ_{floor} and ρ_{ceil}.

Fig. 2 shows the CIRs in the time domain (TD) (Fig. 2a) and the corresponding FDCHTFs (Fig. 2b) of the different channel responses represented in Fig. 1. These curves have been obtained according to (1)-(4) and to the parameters described in the caption of Fig. 2. Observe that the link characterized by the CIR between S and R $\left(h^{\text{SR}}(t)\right)$ and the FD-CHTF $\left|H^{\text{SR}}(f)\right|$ is better than the nLoS CIR and FDCHTF corresponding to the S→D link $\left(h^{\text{SD}}_{\text{nLoS}}(t), \left|H^{\text{SD}}_{\text{nLoS}}(f)\right|\right)$. This means that in case of nLoS propagation, the power received by D from second-order reflections is much lower than the power received by R from S through first-order reflections. Thus, if R is capable of reliably processing the signal gleaned from S, R will forward it and the signal received by D relayed from R will be stronger than in case of no cooperation.

B. IMPLEMENTATION

The proposed reflection-based relaying technique can be established as follows:

1) The user D indicates through the uplink (UL) the index of the AP from which the strongest signal is received. Naturally, it is usually the closest AP which will act as the source S.

2) We stipulate the idealized simplifying assumption that the user has the perfect knowledge of the FDCHTF $\left|H^{\text{SR}}\right| \cdot \left|H^{\text{RD}}\right|$ with respect to the adjacent APs and decides about the best candidate to harness as its relay R. In this first study of wireless backhaul provision the estimation of these quantities is set aside for future research.

3) The user notifies the corresponding AP selected as his/her relay. Furthermore, the user also informs the relay of the source AP identifier.

Following these initialization actions, the reflection-based relaying scenario illustrated in Fig. 1 is set up.

III. DOWNLINK STUDY

As Fig. 1 illustrates, the generic proposal is composed by the cooperative transmission between two APs, one performing as a source S and the other as a relay R, without using any wireline based backhaul link. The signal received by the destination D, is represented by

$$y_D(t) = \eta_{\text{pd,D}} \cdot h_{\text{fe}}(t) \otimes \left(x_S(t) \otimes h^{\text{SD}}_{\text{fs}}(t) + x_R(t) \otimes h^{\text{RD}}_{\text{fs}}(t) \right) + n(t), \tag{6}$$

where $\eta_{\text{pd,D}}$ is the responsivity of the PD at the destination, $h_{\text{fe}}(t)$ is the TD CIR of (2), $x_S(t)$ and $x_R(t)$ are the signals transmitted by S and R in the TD, respectively, and $n(t)$ is the receiver noise in the TD. The noise obeys a zero-mean Gaussian distribution with variance $\sigma_n^2 = \frac{N_0 W}{\xi^2}$, where
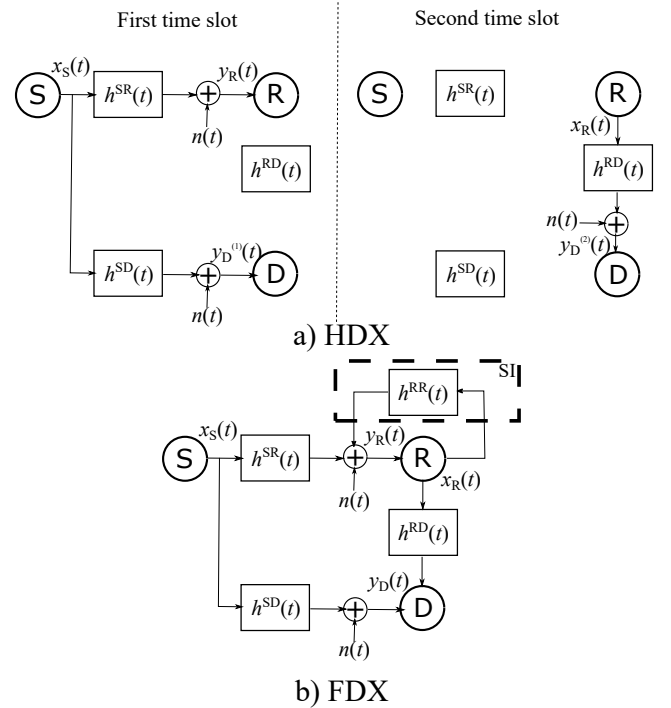

FIGURE 3. Half-duplex and full-duplex cooperative relaying, where the source S transmits a symbol to the destination D.

N_0 is the power spectral density of the noise dominated by the thermal noise in an indoor scenario [6]. Since some subcarriers do not carry energy, a normalization factor ξ is needed to distribute the total transmitted power among the subcarriers carrying energy. If DCO-OFDM is invoked [33], we have $\xi = \sqrt{K/(K-2)}$.

The most popular relaying techniques considered in the literature are [34]:

- Amplify and forward (AF): The relay R receives the signal coming from the source S, amplifies it and forwards it to the destination D.

- Decode and forward (DF): The relay R receives the signal coming from the source S, decodes it and forwards it to the destination D. This technique requires extra signal processing for detecting and channel-decoding the signal, but in exchange, errors can be corrected by the relay.

Furthermore, both of them can be performed in two different modes, as represented in Fig. 3:

- Half duplex (HDX) mode [35]: The cooperation between S and R relies on having two different time slots in Fig. 3. In the first one, S transmits its signal to R and D, leading to $y_D^{(1)}(t)$ at D. The second time slot of Fig. 3 is then utilized by R in order to relay the signal received from S, leading to the signal received by D in the second time slot $y_D^{(2)}(t)$. This mode avoids interference between S as well as R and it makes a low-complexity relay design possible. However, it halves the spectral efficiency. Note that the AF relaying technique

B. Genovés Guzmán *et al.*: Reflection-based Relaying Techniques in Visible Light Communications: Will It Work?

IEEE Access

is capable of operating in HDX mode, as long as a suitable buffer and a switch are installed at R.

- Full duplex (FDX) mode [36]: The relay transmits and receives simultaneously. Thus, it is capable of almost doubling the HDX throughput at the cost of imposing self-interference (SI) owing to leakage of its own transmission into the receiver. This SI has to be cancelled by using interference cancellation techniques. In this paper we study cooperative relaying techniques both with and without SI cancellation and compare their performances.

To make a fair comparison between the HDX and FDX modes, the total electrical transmit power P is shared between S and R. Thus,

- In HDX we have

$$P = P_{\text{S,tx}} = P_{\text{R,tx}}, \tag{7}$$

where $P_{\text{S,tx}}$ and $P_{\text{R,tx}}$ are the transmit power of S and R, respectively.

- In FDX we have

$$P = P_{\text{S,tx}} + P_{\text{R,tx}}, \tag{8}$$

where $P_{\text{S,tx}}$ and $P_{\text{R,tx}}$ are defined:

  – In AF/FDX as follows:

$$P_{\text{S,tx}} = \beta \cdot P, \tag{9}$$

$$P_{\text{R,tx}} = (1 - \beta) \cdot P, \tag{10}$$

  where $\beta \in (0, 1]$ is the power sharing factor.

  – In DF/FDX as follows:

$$P_{\text{S,tx}}[k] = \beta[k] \cdot P/(K - 2), \tag{11}$$

$$P_{\text{R,tx}}[k] = (1 - \beta[k]) \cdot P/(K - 2), \tag{12}$$

  where the power sharing factor of each subcarrier k can be optimized.

In the HDX mode, maximal ratio combining (MRC) [37] [38] [39] may be used upon assuming perfect synchronization. Thus, in both cases the SNR can be expressed as

$$\Gamma_{\text{total},*/\text{HDX}}[k] = \Gamma_{\text{SD},*/\text{HDX}}[k] + \Gamma_{\text{SRD},*/\text{HDX}}[k], \tag{13}$$

where $\Gamma_{\text{SD},*/\text{HDX}}[k]$ is the SNR in HDX mode of the k-th subcarrier received by D from S and $\Gamma_{\text{SRD},*/\text{HDX}}[k]$ is the SNR in HDX mode of the k-th subcarrier received by D coming from the relay path S→R→D. The '*' symbol can be either AF or DF and it is a way to jointly represent both cases. Again, HDX suffers from halving the throughput due to transmission in two time slots per channel use.

Differently, in the FDX mode, by invoking coding techniques [40], and either joint decoding or successive interference cancellation (SIC) techniques [41] [42] for SI rejection, the total SNR can be written as

$$\Gamma_{\text{total},*/\text{FDX}}[k] = \Gamma_{\text{SD},*/\text{FDX}}[k] + \Gamma_{\text{SRD},*/\text{FDX}}[k] - \epsilon, \tag{14}$$

where $\epsilon > 0$ means a decrease in SNR due to not being able to perform MRC. Its value for every case will be given in the following subsections.

A. AMPLIFY AND FORWARD RELAYING

In AF scenarios, the signal transmitted by R is

$$x_{\text{R}}(t) = G_{\text{AF}} \cdot y_{\text{R}}(t), \tag{15}$$

where $G_{\text{AF}} = \sqrt{\frac{P_{\text{R,tx}}}{P_{\text{R,rx}}}}$ is the amplification factor and y_{R} is the signal received by R. Both variables depend on the specific mode invoked,

1) HDX mode

As Fig. 3 shows, in HDX mode $x_{\text{R}}(t)$ is only transmitted in the second time slot per channel use, whereas the first time slot is dedicated for the transmission of $x_{\text{S}}(t)$ by S. In AF/HDX, $y_{\text{R}}(t)$ is composed of the signal $x_{\text{S}}(t)$ transmitted by S in addition to the noise $n(t)$, formulated as

$$y_{\text{R}}(t) = \eta_{\text{pd,R}} \cdot x_{\text{S}}(t) \otimes h_{\text{fs}}^{\text{SR}}(t) \otimes h_{\text{fe}}(t) + n(t), \tag{16}$$

where $\eta_{\text{pd,R}}$ is the responsivity of the relay's PD. Bearing in mind (7), the AF gain can be expressed as

$$G_{\text{AF/HDX}} = \sqrt{\frac{P}{\eta_{\text{pd,R}}^2 \cdot P \cdot \text{E}\left[\left|H_{\text{fs}}^{\text{SR}}[k]\right|^2\right] \cdot \text{E}\left[|H_{\text{fe}}[k]|^2\right] + \sigma_n^2}}, \tag{17}$$

where $\text{E}[\cdot]$ represents the expectation and $P_{\text{R,rx}}$ is the electrical power received by R.

The total SNR formulated in (13) can be expressed by using the SNR of the k-th subcarrier received by D from S, given by

$$\Gamma_{\text{SD,AF/HDX}}[k] = \frac{\eta_{\text{pd,D}}^2 \cdot \xi^2 \cdot P \cdot |H_{\text{fe}}[k]|^2 \cdot \left|H_{\text{fs}}^{\text{SD}}[k]\right|^2}{\sigma_n^2} \tag{18}$$

and the SNR of the k-th subcarrier received by D impinging from the relay path S→R→D, which is formulated as

$$\Gamma_{\text{SRD,AF/HDX}}[k]$$
$$= \frac{\eta_{\text{pd,D}}^2 \xi^2 G_{\text{AF/HDX}}^2 \eta_{\text{pd,R}}^2 P |H_{\text{fe}}[k]|^4 \left|H_{\text{fs}}^{\text{SR}}[k]\right|^2 \left|H_{\text{fs}}^{\text{RD}}[k]\right|^2}{\sigma_n^2 \left(1 + \eta_{\text{pd,D}}^2 |H_{\text{fe}}[k]|^2 \left|H_{\text{fs}}^{\text{RD}}[k]\right|^2 G_{\text{AF/HDX}}^2\right)}. \tag{19}$$

2) FDX mode

In the AF/FDX mode the signal received by R is calculated as

$$y_{\text{R}}(t) = \eta_{\text{pd,R}} \cdot \left(x_{\text{S}}(t) \otimes h_{\text{fs}}^{\text{SR}}(t) + x_{\text{R}}(t) \otimes h_{\text{fs}}^{\text{RR}}(t)\right) \otimes h_{\text{fe}}(t) + n(t), \tag{20}$$

where $x_{\text{R}}(t) \otimes h_{\text{fs}}^{\text{RR}}(t)$ is the SI at R. In this AF/FDX scenario, the AF gain is expressed as

$$G_{\text{AF/FDX}}$$
$$= \sqrt{\frac{(1 - \beta) P}{\eta_{\text{pd,R}}^2 P \left(\beta \text{E}\left[\left|H_{\text{fs}}^{\text{SR}}[k]\right|^2\right] + (1 - \beta) \text{E}\left[\left|H_{\text{fs}}^{\text{RR}}[k]\right|^2\right]\right) \cdot \text{E}\left[|H_{\text{fe}}[k]|^2\right] + \sigma_n^2}}. \tag{21}$$

IEEE *Access*

B. Genovés Guzmán *et al.*: Reflection-based Relaying Techniques in Visible Light Communications: Will It Work?

Thus, the SNR equations needed for computing $\Gamma_{\text{total}}[k]$ indicated in (14) are

$$\Gamma_{\text{SD,AF/FDX}}[k] = \beta\Gamma_{\text{SD,AF/HDX}}[k]$$
$$= \frac{\eta_{\text{pd,D}}^2 \cdot \xi^2 \cdot \beta \cdot P \cdot |H_{\text{fe}}[k]|^2 \cdot |H_{\text{fs}}^{\text{SD}}[k]|^2}{\sigma_n^2} \tag{22}$$

and the one represented in (23) that is located in the following page. The parameter ϵ for this mode is expressed as (24), also located in next page. Due to the low value of ϵ, it can be assumed as negligible for our scenario.

B. DECODE AND FORWARD RELAYING
In DF, the signal transmitted by R is defined as

$$x_{\text{R}}(t) = \hat{x}_{\text{S}}(t), \tag{25}$$

where $\hat{x}_{\text{S}}(t)$ is a result of decoding and processing the signal $x_{\text{S}}(t)$ transmitted by S. Note that the signals received by R in the DF/HDX and DF/FDX modes are the same as in AF/HDX and AF/FDX, which were defined in (16) and (20), respectively. Again, the SNR equations depend on the transmission mode:

1) HDX mode
Recall that in the HDX mode there is no interference between $x_{\text{S}}(t)$ and $x_{\text{R}}(t)$ due to using different time slots. In DF/HDX, the SNR of the S→D link is the same as in the AF/HDX case:

$$\Gamma_{\text{SD,DF/HDX}}[k] = \Gamma_{\text{SD,AF/HDX}}[k]. \tag{26}$$

By contrast, the SNR of the signal received by D arriving from the relay path S→R→D is determined by the weaker of the independent S→R and R→D links as [43] [44].

$$\Gamma_{\text{SRD,DF/HDX}}[k] = \min\left(\Gamma_{\text{SR,DF/HDX}}[k], \Gamma_{\text{RD,DF/HDX}}[k]\right). \tag{27}$$

Due to using two different time slots for the transmission of S and R, no SI is present in the HDX mode and the SNR of the link between S and R is obtained from (16) as

$$\Gamma_{\text{SR,DF/HDX}}[k] = \frac{\eta_{\text{pd,R}}^2 \cdot \xi^2 \cdot P \cdot |H_{\text{fe}}[k]|^2 \cdot |H_{\text{fs}}^{\text{SR}}[k]|^2}{\sigma_n^2}, \tag{28}$$

whereas the SNR of the link between R and D is formulated as

$$\Gamma_{\text{RD,DF/HDX}}[k] = \frac{\eta_{\text{pd,D}}^2 \cdot \xi^2 \cdot P \cdot |H_{\text{fe}}[k]|^2 \cdot |H_{\text{fs}}^{\text{RD}}[k]|^2}{\sigma_n^2}. \tag{29}$$

2) FDX mode
In DF/FDX, the SNR of the S→D link can be expressed as

$$\Gamma_{\text{SD,DF/FDX}}[k] = \beta[k] \cdot \Gamma_{\text{SD,DF/HDX}}[k]$$
$$= \Gamma_{\text{SD,AF/FDX}}[k]. \tag{30}$$

Again, the SNR of the S→R→D relaying link is formulated as

$$\Gamma_{\text{SRD,DF/FDX}}[k] = \min\left(\Gamma_{\text{SR,DF/FDX}}[k], \Gamma_{\text{RD,DF/FDX}}[k]\right), \tag{31}$$

where $\Gamma_{\text{SR,DF/FDX}}[k]$ and $\Gamma_{\text{RD,DF/FDX}}[k]$ are the SNR in the k-th subcarrier in the links S→R and R→D, respectively, when the DF/FDX technique is employed. In the presence of SI, the SNR of the S→R link is obtained from (20) by

$$\Gamma_{\text{SR,DF/FDX}_{\text{SI}}}[k] \approx \frac{\eta_{\text{pd,R}}^2 \xi^2 \beta[k] P |H_{\text{fe}}[k]|^2 |H_{\text{fs}}^{\text{SR}}[k]|^2}{\sigma_n^2 + \eta_{\text{pd,R}}^2 \xi^2 (1-\beta[k]) P |H_{\text{fe}}[k]|^2 |H_{\text{fs}}^{\text{RR}}[k]|^2}. \tag{32}$$

By contrast, this SNR is considerably improved if perfect SI cancellation is achieved, yielding

$$\Gamma_{\text{SR,DF/FDX}_{\text{nSI}}}[k] \approx \frac{\eta_{\text{pd,R}}^2 \xi^2 \beta[k] P |H_{\text{fe}}[k]|^2 |H_{\text{fs}}^{\text{SR}}[k]|^2}{\sigma_n^2}. \tag{33}$$

In both cases, the SNR of the R→D link is given by

$$\Gamma_{\text{RD,DF/FDX}}[k] \approx \frac{\eta_{\text{pd,D}}^2 \xi^2 (1-\beta[k]) P |H_{\text{fe}}[k]|^2 |H_{\text{fs}}^{\text{RD}}[k]|^2}{\sigma_n^2}. \tag{34}$$

Note that, if SI cancellation techniques are invoked, $\epsilon \approx 0$. Differently, when SI is not cancelled at R and $\Gamma_{\text{SR,DF/FDX}_{\text{SI}}}[k] < \Gamma_{\text{RD,DF/FDX}}[k]$,

$$\epsilon_{\text{DF/FDX}} \approx \frac{\beta[k]\eta_{\text{pd,D}}^2 \cdot \xi^2 \cdot P \cdot |H_{\text{fe}}[k]|^2 \cdot |H_{\text{fs}}^{\text{SD}}[k]|^2}{\sigma_n^2}$$
$$- \frac{\beta[k]\eta_{\text{pd,D}}^2 \cdot \xi^2 \cdot P \cdot |H_{\text{fe}}[k]|^2 \cdot |H_{\text{fs}}^{\text{SD}}[k]|^2}{\sigma_n^2 + \eta_{\text{pd,R}}^2 \xi^2 (1-\beta[k]) P |H_{\text{fe}}[k]|^2 |H_{\text{fs}}^{\text{RR}}[k]|^2}, \tag{35}$$

which is negligible for the total SNR calculation.

IV. SYSTEM ANALYSIS
To focus our study, we have to choose between AF and DF to attain the best performance in our application, which is expressed as

$$\underset{\text{AF, DF}}{\arg\max} \, \Gamma_{\text{total}}[k], \tag{36}$$

where $\Gamma_{\text{total}}[k]$ is formulated in (13). This expression is valid for both the FDX and HDX modes, provided that the SI is successfully cancelled as previously indicated. It will be determined by comparing

$$\Gamma_{\text{total,AF/*}}[k] = \Gamma_{\text{SD,AF/*}}[k] + \Gamma_{\text{SRD,AF/*}}[k] \tag{37}$$

B. Genovés Guzmán *et al.*: Reflection-based Relaying Techniques in Visible Light Communications: Will It Work?

IEEE *Access*

$$\Gamma_{\text{SRD,AF/FDX}}[k] = \frac{\xi^2 \eta_{\text{pd,R}}^2 \beta P |H_{\text{fe}}[k]|^2 |H_{\text{fs}}^{\text{SR}}[k]|^2}{\sigma_n^2 \left(\frac{1}{\eta_{\text{pd,D}}^2 G_{\text{AF/FDX}}^2 |H_{\text{fs}}^{\text{RD}}[k]|^2 |H_{\text{fe}}[k]|^2} + 1 \right) + \eta_{\text{pd,R}}^2 (1-\beta) P |H_{\text{fs}}^{\text{RR}}[k]|^2 |H_{\text{fe}}[k]|^2}. \tag{23}$$

$$\epsilon_{\text{AF/FDX}} = \frac{\xi^2 \eta_{\text{pd,D}}^2 \beta P |H_{\text{fe}}[k]|^2 |H_{\text{fs}}^{\text{SD}}[k]|^2}{\sigma_n^2} - \frac{\xi^2 \eta_{\text{pd,D}}^2 \beta P |H_{\text{fe}}[k]|^2 |H_{\text{fs}}^{\text{SD}}[k]|^2}{\sigma_n^2 + \eta_{\text{pd,D}}^2 |H_{\text{fe}}[k]|^2 G_{\text{AF/FDX}}^2 \left(\eta_{\text{pd,R}}^2 (1-\beta) P |H_{\text{fs}}^{\text{RR}}[k]|^2 |H_{\text{fe}}[k]|^2 + \sigma_n^2 \right) |H_{\text{fs}}^{\text{RD}}[k]|^2}. \tag{24}$$

and

$$\Gamma_{\text{total,DF/*}}[k] = \Gamma_{\text{SD,DF/*}}[k] + \Gamma_{\text{SRD,DF/*}}[k], \tag{38}$$

where '*' represents either HDX or FDX. As seen in (26) and (30), we have $\Gamma_{\text{SD,AF/*}}[k] = \Gamma_{\text{SD,DF/*}}[k]$. Thus, (36) can be simplified to

$$\underset{\text{AF, DF}}{\arg \max} \; \Gamma_{\text{SRD}}[k]. \tag{39}$$

In HDX, according to (19), (27), (28) and (29) we have $\Gamma_{\text{SRD,AF/HDX}}[k] \leq \Gamma_{\text{SRD,DF/HDX}}[k]$, because $\Gamma_{\text{SRD,AF/HDX}}[k] \leq \Gamma_{\text{SR,DF/HDX}}[k]$ and $\Gamma_{\text{SRD,AF/HDX}}[k] \leq \Gamma_{\text{RD,DF/HDX}}[k]$. Additionally, in FDX, by comparing (23) to (31), (32), (33) and (34), note that $\Gamma_{\text{SRD,AF/FDX}}[k] \leq \Gamma_{\text{SRD,DF/FDX}}[k]$. Thus, we conclude that DF offers a better performance than AF, both in the HDX and FDX mode. Hence, from now on, the study focuses on the DF relaying technique.

Recall from Section III-B that the FDX mode requires the system to share the total available power P between S and R, as indicated by (11) and (12). The power sharing factor between S and R is denoted by $\beta[k]$ and the optimum value in DF/FDX is given by

$$\beta_{\text{opt}_{\text{DF/FDX}}}[k] = \begin{cases} 1, & \text{if LoS in S} \rightarrow \text{D link} \\ \beta_{\text{th}_{\text{DF/FDX}}}[k], & \text{if nLoS in S} \rightarrow \text{D link} \end{cases}. \tag{40}$$

The proof of (40) is given in Appendix A and $\beta_{\text{th}_{\text{DF/FDX}}}[k]$ is provided in Appendix B.

Typically, cooperative communication is managed by a central entity, which processes and distributes the data using a wired backhaul to allocate and transmit data through different APs. As an upper bound, we also want to characterize the wired backhaul by optimizing its power sharing factor β_{bh} and comparing it to our proposed solution. The total SNR of a wired backhaul-based cooperative scheme is formulated by

$$\Gamma_{\text{total,bh}}[k]$$
$$\approx \frac{\eta_{\text{pd,D}}^2 \xi^2 P |H_{\text{fe}}[k]|^2 \left| \sqrt{\beta_{\text{bh}}[k]} H_{\text{fs}}^{\text{SD}}[k] + \sqrt{1 - \beta_{\text{bh}}[k]} H_{\text{fs}}^{\text{RD}}[k] \right|^2}{\sigma_n^2}, \tag{41}$$

which is maximized upon using a $\beta_{\text{opt,bh}}[k]$ value of

$$\beta_{\text{opt,bh}}[k] = \left(1 + \frac{|H_{\text{fs}}^{\text{RD}}[k]|^2}{|H_{\text{fs}}^{\text{SD}}[k]|^2} \right)^{-1}. \tag{42}$$

Naturally, the optimal power sharing depends on the channels between the APs and the user.

Fig. 4 represents the optimal value of β against the ratio between the horizontal length of the SD and RD links. For the sake of simplicity, only results for $k = 1$ are represented, although the total electrical bandwidth is divided into $K = 512$ frequency subcarriers. Note that an SNR comparison considering any other subcarrier would reflect similar relative SNR trends to those seen in Fig. 4, due to the pass filtering effects imposed by the FDCHTF that affect all techniques similarly. The results of the following six schemes representing different backhaul techniques are discussed:

a (b): wired backhaul and LoS (nLoS) propagation between S and D.

c (d): DF/FDX-based wireless backhaul in the presence of SI, when we have LoS (nLoS) propagation between S and D.

e (f): DF/FDX-based wireless backhaul with perfect SI cancellation, when we have LoS (nLoS) propagation between S and D.

The parameters used are the same as the ones indicated in Fig. 2. For the wired backhaul case when there is LoS between S and D (Fig. 4a), note that the closer the user D to R, the lower β_{opt} becomes, which means that a higher power must be allocated to R. When D is exactly at the midpoint of S and R, equal power allocation (EPA) must be used between S and R ($\beta_{\text{opt}} = 0.5$) in order to maximize the SNR at D. When nLoS propagation prevails in the wired backhaul solution (Fig. 4b), most of the power must be transmitted by R. Note that still non-zero power ($\beta_{\text{opt}} \approx 0.1$) is allocated to S when D is close to it, because at that location the signal power transmitted from S and received through reflections is substantial.

By contrast, when the DF/FDX technique is employed in a LoS scenario (Fig. 4c and Fig. 4e), no cooperation is recommended because the information arriving at R through the reflected relay path (S→R) is rather degraded. Thus, it is better to assign all the power to S. When the S→D path is blocked and no SI cancellation is employed (Fig. 4d), most of the power must still be assigned to S, because the SI signal received by R from its own transmission is harmful. However, when the SI is cancelled in R and the S→D path is blocked (Fig. 4f), most of the power must be assigned to R. The higher the distance ratio, the closer D to R, which allows the power transmitted by R to be reduced in favor of increasing the
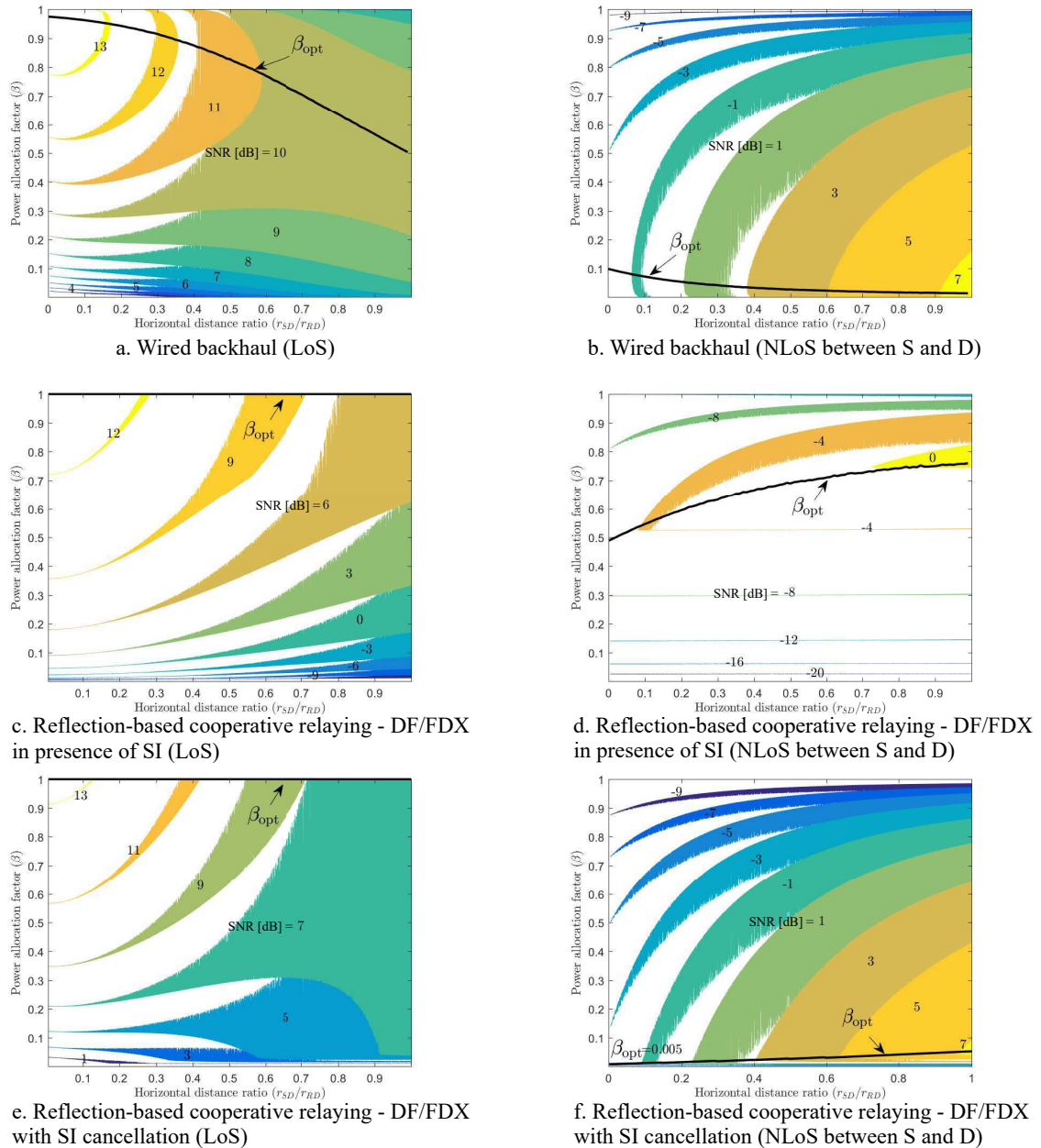
IEEE Access

B. Genovés Guzmán *et al.*: Reflection-based Relaying Techniques in Visible Light Communications: Will It Work?

FIGURE 4. Representation of the optimum power sharing factor (β_{opt}) for $k = 1$ against the horizontal distance ratio that determines the user location when a wired backhaul (a)-(b), DF/FDX cooperative-relaying in presence of SI (c)-(d) or DF/FDX cooperative-relaying with perfect SI cancellation (e)-(f) are employed. Also, SNR [dB] values for every β and $r_{\mathrm{SD}}/r_{\mathrm{RD}}$ are represented.

power transmitted by S. As a consequence, this improves the quality of the S→R path. By comparing Fig. 4d and Fig. 4f, we realize how important it is to perform SI cancellation at R, because a gain of around 7 dB can be obtained.

In general, a higher SNR is attained by the wired backhaul solution, which hence constitutes an upper bound. However, if near-perfect SI cancellation is carried out, a performance close to that obtained by the wired solution can be achieved (see Fig.4a-Fig. 4e and Fig.4b-Fig. 4f). Quantitatively, a maximum SNR of around 13 dB and 7 dB can be obtained, when there is LoS and nLoS propagation between S and D, respec-

tively, for both the wired backhaul and for DF/FDX relying on perfect SI cancellation. Note that SI cancellation is indeed feasible because the relay knows the previous transmitted symbol and the SI is only produced by the reflection of the floor.

V. SQUARE-SHAPED LIFI ATTOCELLS
The most common LiFi network model is the square-shaped tessellation based one, where the APs are distributed on a square lattice, as shown in Fig. 5. It provides uniform illumination distribution and it is eminently suitable for
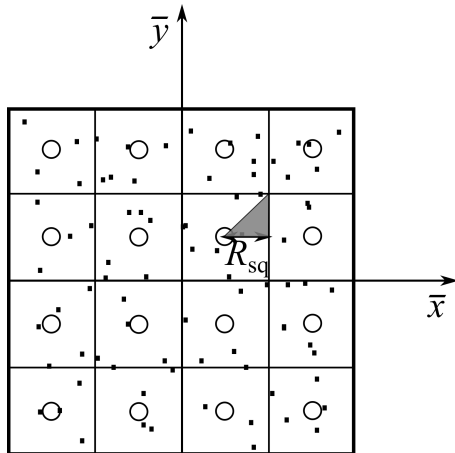
B. Genovés Guzmán *et al.*: Reflection-based Relaying Techniques in Visible Light Communications: Will It Work?

IEEE *Access*

FIGURE 5. Square tessellation model.

rectangular-shaped rooms. Hence, this study investigates this scenario.

In reality, only the discrete-input continuous-output memoryless channel (DCMC) capacity can be achieved by practical discrete modulation schemes [38]. Explicitly, when using adaptive modulation and coding schemes (AMC), the SNR range is divided into $(L+1)$ channel quality regions $\Re_l = \{\gamma_{\text{th}}[l], \gamma_{\text{th}}[l+1]\}$, $l = 0, 1, ..., L$ with $\gamma_{\text{th}}[0] = 0$ and $\gamma_{\text{th}}[L+1] = \infty$. For each region $\Re_l$, a certain constellation/coding scheme can be employed for transmitting $\epsilon[l]$ bits/symbol. Below $\gamma_{\text{th}}[1]$ no transmission is possible and the system is said to be in outage. By contrast, above $\gamma_{\text{th}}[L]$ the maximum throughput is attained and no rate improvement is possible with this AMC scheme.

The switching thresholds between the constellations $\{\gamma_{\text{th}}[l]\}_{l=1,..,L}$ are established to satisfy the BER target of the system [38]. The AMC throughput can be written as a function of the SNR as

$$\eta_{\text{AMC}} = \epsilon[l], \qquad \text{SNR} \in [\gamma_{\text{th}}[l], \gamma_{\text{th}}[l+1]]. \tag{43}$$

For a certain average SNR Γ, the average throughput under AMC can be expressed as

$$E[\eta_{AMC}] = \sum_{l=1}^{L} \epsilon[l] \cdot \Pr\{\gamma_{\text{th}}[l] \leq \Gamma < \gamma_{\text{th}}[l+1]\}$$
$$= \sum_{l=1}^{L} \epsilon[l] \cdot [F_\Gamma(\gamma_{\text{th}}[l+1]) - F_\Gamma(\gamma_{\text{th}}[l])], \tag{44}$$

where $F_\Gamma(\gamma_{\text{th}})$ is the cumulative density function (CDF) of the SNR evaluated in terms of γ_{th} expressed as

$$F_\Gamma(\gamma_{\text{th}}) = \Pr\{\Gamma[k] < \gamma_{\text{th}}\}$$
$$= \int_0^{R_{\text{sq}}} f_Y(y) \cdot \Pr\{\Gamma[k] < \gamma_{\text{th}}|y\} dy, \tag{45}$$

where x and y are the Cartesian coordinates of D with respect to the AP under study. Since the users are uniformly

distributed in the cell, the joint probability density function of X and Y is

$$f_{X,Y}(x,y) = f_{X|Y}(x|y) \cdot f_Y(y)$$
$$= \frac{1}{R_{\text{sq}} - y} \cdot \frac{1}{R_{\text{sq}}}, \quad x \in [y, R_{\text{sq}}], \ y \in [0, R_{\text{sq}}], \tag{46}$$

where $2 \cdot R_{\text{sq}}$ represents the edge-length of the square-shaped cell, as indicated in Fig. 5. Thanks to the geometry of the system, the study of the shaded region in Fig. 5 is representative of the whole network, as long as the room is large enough.

If the S→D link exhibits LoS propagation, we have $\beta_{\text{opt}_{\text{DF/FDX}}}[k] = 1 \forall k$. Then, with the aid of (4) and (30), the total SNR in DF/FDX can be formulated as

$$\Gamma_{\text{total}_{\text{DF/FDX}}}[k]\Big|_{\text{LoS in S→D}} = \Gamma_{\text{single}}[k]$$
$$= \frac{U}{(x^2+y^2+d_{\text{v}}^2)^{m+3}}, \tag{47}$$

where $\Gamma_{\text{single}}[k]$, expressed as in (18), represents the SNR obtained when a single transmission from S to D takes place, while

$$U = \frac{\eta_{\text{pd,D}}^2 \xi^2 P \left|H_{\text{fe}}[k]\right|^2 (m+1)^2 G_f^2 G_c^2 A_{\text{r}}^2 d_{\text{v}}^{2m+2}}{4\pi^2 \sigma_n^2}, \tag{48}$$

where all the variables were defined previously. Thus, we arrive at

$$\Pr\left\{\Gamma_{\text{total}_{\text{DF/FDX}}}[k]\Big|_{\text{LoS in S→D}} < \gamma_{\text{th}}\Big|Y\right\}$$
$$= \Pr\left\{X^2 > \left(\frac{U}{\gamma_{\text{th}}}\right)^{1/(m+3)} - y^2 - d_{\text{v}}^2\Big|Y\right\}$$
$$= 1 - \frac{\sqrt{\left(\frac{U}{\gamma_{\text{th}}}\right)^{1/(m+3)} - y^2 - d_{\text{v}}^2} - y}{R_{\text{sq}} - y}. \tag{49}$$

The CDF of the SNR, in case of DF/FDX and LoS in the S→D link, can finally be calculated as

$$\Pr\left\{\Gamma_{\text{total}_{\text{DF/FDX}}}[k]\Big|_{\text{LoS in S→D}} < \gamma_{\text{th}}\right\}$$
$$= \int_0^{R_{\text{sq}}} \frac{1}{R_{\text{sq}}} \cdot \Pr\left\{\Gamma_{\text{total}_{\text{DF/FDX}}}[k]\Big|_{\text{LoS in S→D}} < \gamma_{\text{th}}\Big|Y\right\} dy. \tag{50}$$

When DF/FDX is used and the S→D link exhibits nLoS propagation, or the wired backhaul solution is employed, $F_\Gamma(\gamma_{\text{th}})$ can be obtained by numerical methods following the same reasoning as before.

Upon using AMC schemes as defined in (43), the spectral efficiency (SE) is expressed as

$$\text{SE} = \frac{1}{K} \sum_{k=1}^{\frac{K}{2}-1} \sum_{l=1}^{L} \epsilon[l] \left(\Pr\{\Gamma[k] < \gamma_{\text{th}}[l+1]\} - \Pr\{\Gamma[k] < \gamma_{\text{th}}[l]\}\right), \tag{51}$$

IEEE *Access*

B. Genovés Guzmán *et al.*: Reflection-based Relaying Techniques in Visible Light Communications: Will It Work?

TABLE 1. System Parameters

Parameter	Value	Unit
Half of the squared cell's edge-length, R_{sq}	1.5	[m]
Vertical distance between AP and user, d_{v}	2.25	[m]
Total electrical power, P	4.7	[W]
Half-power semi-angle, $\phi_{1/2}$	60	[°]
Modulation bandwidth, W	280	[MHz]
Number of subcarriers, K	512	
Front-end device bandwidth factor, F_{fe}	35.6	[MHz]
Relay's PD responsivity, $\eta_{\text{pd,R}}$	16	[A/W]
User's PD responsivity, $\eta_{\text{pd,D}}$	0.4	[A/W]
PD physical area, A_{r}	8.72	[mm^2]
Receiver field of view, Ψ_{FoV}	90	[°]
Optical filter loss, G_{f}	1	
Refractive index of concentrator, n_{ref}	1.5	
UE density, λ_{ue}	0.1	[user/m^2]
Blocker density, λ_{b}	0.1	[user/m^2]
Reflectance factor of ceiling, ρ_{ceil}	0.8	
Reflectance factor of floor, ρ_{floor}	0.6	
Noise power spectral density, N_0	10^{-21}	[A^2/Hz]

TABLE 2. Adaptive Modulation and Coding SINR regions

$\gamma_{\text{th}}[l]$ [dB]	Modulation	Code rate	$\epsilon[l]$ [bits/symbol]
-6 ($\gamma_{\min}$)	QPSK	0.076	0.1523
-5	QPSK	0.117	0.2344
-3	QPSK	0.188	0.3770
-1	QPSK	0.301	0.6016
1	QPSK	0.438	0.8770
3	QPSK	0.588	1.1758
5	16QAM	0.369	1.4766
8	16QAM	0.476	1.9141
9	16QAM	0.602	2.4063
11	64QAM	0.455	2.7305
12	64QAM	0.554	3.3223
14	64QAM	0.650	3.9023
16	64QAM	0.754	4.5234
18	64QAM	0.853	5.1151
20	64QAM	0.926	5.5547

which is halved when the HDX mode is employed.

An additional metric of evaluating how the performance varies among users is the popular Jain index of fairness [45] formulated by

$$F_J = \frac{\left(\sum_{i=1}^{N_{\text{ue}}} \text{SE}_i\right)^2}{N_{\text{ue}} \cdot \sum_{i=1}^{N_{\text{ue}}} \text{SE}_i^2}, \qquad (52)$$

where N_{ue} is the number of users within a cell.

VI. PERFORMANCE RESULTS

To evaluate the performance results, the popular parameters of a VLC system are used, which are summarised in Table 1 [46]. The simulation parameters are described in Table 1. A realistic scenario associated with dimensions of 12 x 12 x 3 m is considered with a square tessellation model, as represented in Fig. 5, where $2 \cdot R_{\text{sq}}$ denotes the length of a squared-shaped cell's edge. A DCO-OFDM transmission scheme is used. The front-end device bandwidth factor F_{fe} is 35.6 MHz, assuming the use of LED in [47]. The number of UEs, each of them associated with a person, is modeled by the variable λ_{ue}, whereas the number of additional people without a UE who constitute blockers is denoted by λ_{b}. Every person is approximated by a cylinder of a 0.15 m radius and a height of 1.75 m [48]. The UE is located at a distance of 0.3 m separated from the associated human body, and the azimuth angle follows a uniform distribution $\mathcal{U}(0, 2\pi)$. The reflectance factors depend on the materials, colors and finishes that are employed on the surfaces. The typical values of $[\rho_{\text{ceil}}; \rho_{\text{floor}}] = [0.8; 0.6]$ are selected in this work [49] [50]. A spectrally efficient AMC is considered [51], whose operating regions are displayed in Table 2.

Fig. 6 represents the SNR when using different transmission schemes:

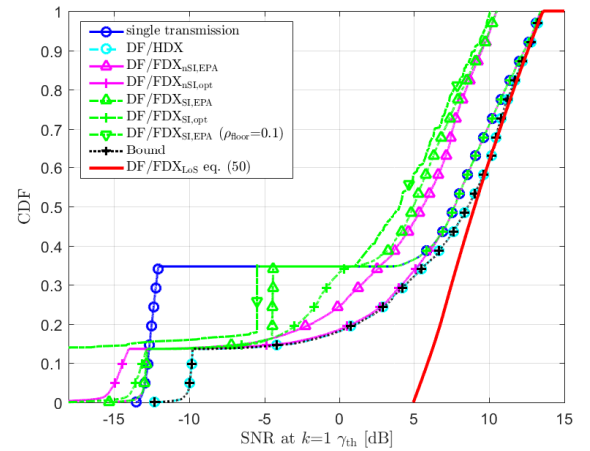- Scheme 1: Single-hop transmission.
- Scheme 2: DF/HDX.

FIGURE 6. Cumulative Distribution Function of the SNR at subcarrier index $k = 1$ for different schemes with $\lambda_{\text{b}} = 0.1$. The DF/FDX$_{\text{LoS}}$ analytical results were calculated from (50).
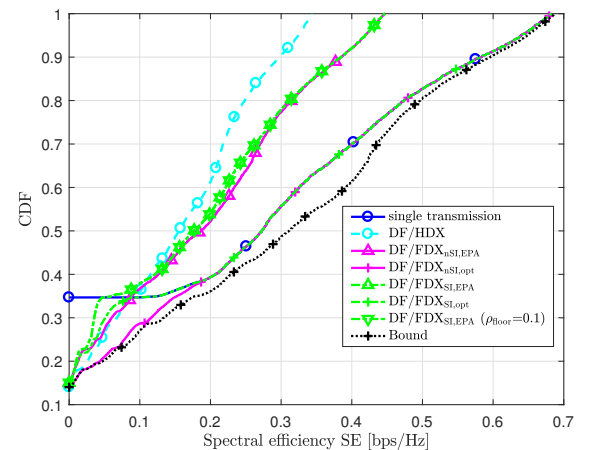

FIGURE 7. Cumulative Distribution Function of the spectral efficiency for different schemes.

- Scheme 3: DF/FDX with perfect SI cancellation and an equal power allocation (DF/FDX$_{\text{nSI,EPA}}$).

B. Genovés Guzmán *et al.*: Reflection-based Relaying Techniques in Visible Light Communications: Will It Work?

IEEE *Access*

- Scheme 4: DF/FDX with perfect SI cancellation and an optimum power allocation (DF/FDX$_{\text{nSI,opt}}$).
- Scheme 5: DF/FDX with no SI cancellation and an equal power allocation (DF/FDX$_{\text{SI,EPA}}$).
- Scheme 6: DF/FDX with no SI cancellation and an optimum power allocation (DF/FDX$_{\text{SI,opt}}$).
- Scheme 7: Traditional wired backhaul solution in conjunction with an optimum power allocation (upper bound). Note that this scheme was mathematically presented in (41) and (42).

For the sake of simplicity, only results for the first subcarrier that transports data ($k = 1$) are represented. Note that the DF/FDX$_{\text{SI,EPA}}$ scheme is also characterized for $\rho_{\text{floor}} = 0.1$ as the worst case scenario, where the material of the floor barely reflects the light. In this case, D that suffers from nLoS propagation with both S and R experiences extremely low SNR values, because the power gleaned from second-order reflections is very low. As a consequence, the users are in outage. The DF/HDX scheme provides similar SNR performance in Fig. 6 to the upper bound, since the maximum available power is used by every AP, whilst relying on two time slots. Both DF/FDX$_{\text{nSI,opt}}$ and DF/FDX$_{\text{SI,opt}}$ are seen in Fig. 6 to offer a performance close to the upper bound at high SNR values, in which case there is LoS propagation between S and D and then non-relayed transmission corresponds to the optimum power allocation. By contrast, the SNR performance of DF/FDX$_{\text{nSI,EPA}}$ and DF/FDX$_{\text{SI,EPA}}$ degrades by about 3 dB at high SNR values compared to the upper bound. Most of the CDF curves exhibit degradation at some SNR value, in the event of a LoS-link blockage with respect to both serving APs (or the only AP in the non-relaying transmission mode). The higher the SNR, the closer the curves appear to be to the upper bound. Additionally, the simulation results closely match the analytical DF/FDX$_{\text{LoS}}$ curve of (50), which verifies the analytical results obtained in Section V. The lower the SNR value, the higher the number of users that experience a LoS-link blockage between S and D, hence the higher the differences with respect to the analytical DF/FDX$_{\text{LoS}}$ curve become.

Fig. 7 represents the CDF of the spectral efficiency computed from (51). Again, single transmission dispensing with relaying can offer the best performance for users who experience LoS propagation. However, a zero-spectral efficiency, which is equivalent to the outage probability, is obtained with a 35% probability. By contrast, the rest of the schemes reduce this outage probability to 15%, which means that the use of cooperative schemes in indoor VLC scenarios may be deemed beneficial. Note that these probabilities are the same as the percentage of users that experience nLoS in Fig. 6 and suffer from a high SNR degradation. The DF/FDX$_{\text{nSI,opt}}$ approaches the upper bound, whereas DF/HDX suffers from halving the spectral efficiency because of using two time slots per transmission. Note that the difference in SNR when a non-reflective flooring material is used is not substantial in terms of spectral efficiency, provided that an AMC is used.
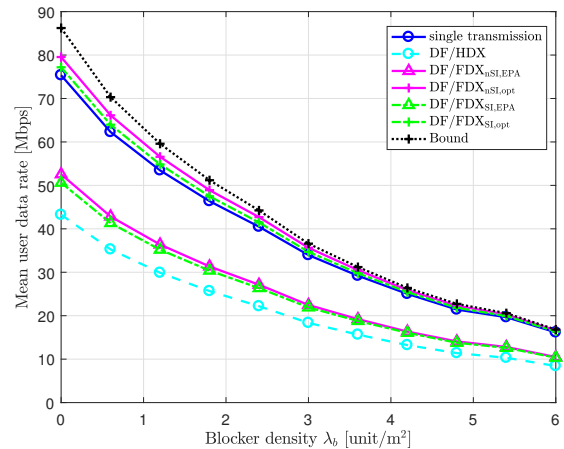
Fig. 8 shows the mean user data rate computed from (51)

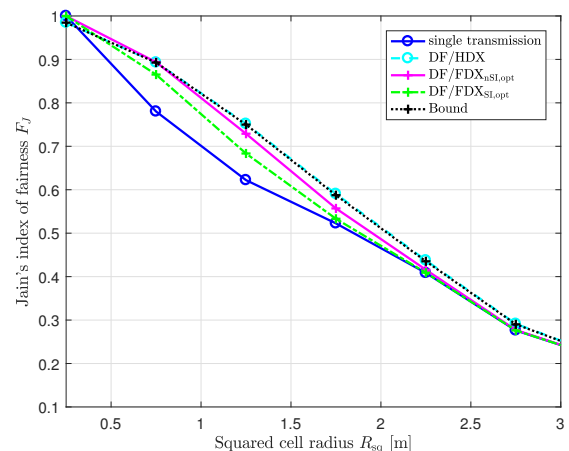**FIGURE 8.** Mean user data rate vs. blocker density.

FIGURE 9. Jain's index of fairness vs. cell radius for different schemes.

and multiplied by the total bandwidth, when it is supposed to have a single user per source-relay association, upon varying the blocker density. As expected, the higher the blocker density, the lower the mean user data rate, potentially approaching a scenario where only reflections arrive to the destination. In this extreme situation, all curves converge, because the performance degradation is similar in all cases. In cases where λ_{b} is low, we note that the proposed scheme approaches the upper bound (wired traditional scheme) if both SI cancellation and an optimum power allocation are employed. However, the EPA schemes attain lower performances. The DF/HDX scheme, despite guaranteeing the best SNR, suffers from throughput-halving, since two time slots per channel-use are employed.

The reflection-based cooperative schemes offer a fairer data rate performance, as Fig. 9 shows. The proposed reflection-based scheme relying on SI cancellation approaches the upper bound represented by the traditional wired backhaul scheme. As expected, the higher the cell
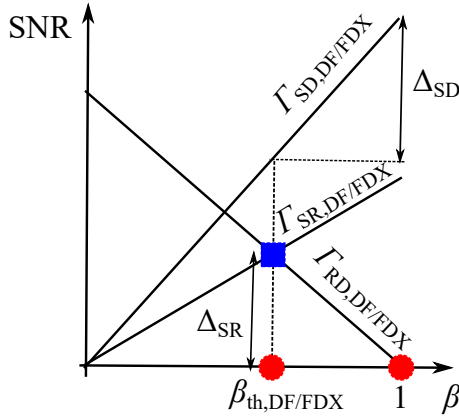
IEEE *Access*

B. Genovés Guzmán *et al.*: Reflection-based Relaying Techniques in Visible Light Communications: Will It Work?

FIGURE 10. Exemplification of SNR curves for different links to demonstrate the optimal β values in DF/FDX mode.

radius, the higher the differences between the users served within the same cell and, as a consequence, the lower Jain's index of fairness becomes. Note that, when the radius is high, all the techniques are equally affected.

VII. CONCLUSIONS

This paper proposed an alternative solution to an ordinary wired backhaul system. Since the wired system involves cumbersome installation, an ad-hoc wireless backhaul system that hardly modifies the existing infraestructure, whilst achieving a similar performance is proposed. This system relies on reflections from the floor for conveying information to the neighboring APs that act as relays. The AF and DF relaying techniques were evaluated using both FDX and HDX transmission modes. It was demonstrated that this system, operating in the DF/FDX mode, achieves a similar SNR (with a difference of around 1 dB) and data rate to the wired backhaul system, as long as an optimum power-sharing and perfect SI cancellation techniques are employed at the relay. By contrast, if an equal power allocation is performed between the source and the relay, the system degrades around 3 dB at high SNR values. The blocker density affects equally both the conventional wired and the proposed wireless systems, with a negligible difference of around 5 Mbps of mean user data rate at low blocker density values. Both analytical as well as simulation results were presented and, as mentioned, the data rate, spectral efficiency and JainâĂŹs index of fairness were evaluated. Finally, responding to the question posed in the title, the proposed reflection-based relaying technique may be expected to perform well in LiFi scenarios. However, when implementing this approach, the associated reflectance values and signal processing techniques at both the relay and destination nodes should be carefully considered. Finally, the processing time delay at the relay and destination will be studied in our further work by considering a twin-component objective function for both the SNR and delay variables, as well as the throughput.

.

APPENDIX A PROOF OF (40)

According to (30), (32), (33) and (34), the SNR values for links S→D and S→R are increasing with β, whereas the SNR for the R→D link decreases. These functions are exemplified in Fig. 10. Recall from (38), that $\Gamma_{\text{total,DF/FDX}}[k] = \Gamma_{\text{SD,DF/FDX}}[k] + \min\left(\Gamma_{\text{SR,DF/FDX}}[k], \Gamma_{\text{RD,DF/FDX}}[k]\right)$. Note that $\beta_{\text{th}_{\text{DF/FDX}}}$ maximizes the function $\min(\Gamma_{\text{SR,DF/FDX}}[k], \Gamma_{\text{RD,DF/FDX}}[k])$, whose value is highlighted by a blue square.

Fig. 10 establishes the only two possible solutions, highlighted by red circles, for $\beta_{\text{opt}} = \arg\max_\beta \Gamma_{\text{total,DF/FDX}}[k]$, which are

$$\beta_{\text{opt}_{\text{DF/FDX}}}[k] = \begin{cases} 1, & \text{if } \Delta_{\text{SD}} > \Delta_{\text{SR}} \\ \beta_{\text{th}_{\text{DF/FDX}}}[k], & \text{if } \Delta_{\text{SD}} \leq \Delta_{\text{SR}} \end{cases}, \quad (53)$$

where $\Delta_{\text{SD}} = \tan\left|\frac{\partial\Gamma_{\text{SD,DF/FDX}}[k]}{\partial\beta}\right| \cdot (1 - \beta_{\text{th}})$ is the SNR increase in the S→D link, when β goes from $\beta_{\text{th}_{\text{DF/FDX}}}$ to 1. And $\Delta_{\text{SR}} = \max\left(\min\left(\Gamma_{\text{SR,DF/FDX}}[k], \Gamma_{\text{RD,DF/FDX}}[k]\right)\right) = \tan\left|\frac{\partial\Gamma_{\text{RD,DF/FDX}}[k]}{\partial\beta}\right| \cdot (1 - \beta_{\text{th}})$. According to (30) as well as (34) and since the LoS distance between S and D is shorter than the distance between R and D, $\Delta_{\text{SD}} \leq \Delta_{\text{SR}}$ is only satisfied when there is no LoS-link between S and D. Thus, (53) is equivalent to (40).

APPENDIX B DERIVATION OF $\beta_{\text{th}_{\text{DF/FDX}}}[k]$

The $\beta_{\text{th}_{\text{DF/FDX}}}[k]$ value is obtained by equating (34) and (32) in presence of SI, and (34) and (33) when a perfect SI cancellation is assumed. In the first case,

$$\beta_{\text{th}_{\text{DF/FDX,SI}}}[k] = 1 + \frac{BC + A - \sqrt{4BFA + (BC + A)^2}}{2BF}, \quad (54)$$

$$A = \eta_{\text{pd,R}}^2 \left|H_{\text{fs}}^{\text{SR}}[k]\right|^2 \sigma_{\text{n}}^2, \quad (55)$$

$$B = \eta_{\text{pd,D}}^2 \left|H_{\text{fs}}^{\text{RD}}[k]\right|^2, \quad (56)$$

$$C = \sigma_{\text{n}}^2, \quad (57)$$

$$F = \eta_{\text{pd,R}}^2 P \left|H_{\text{fe}}[k]\right|^2 \left|H_{\text{fs}}^{\text{RR}}[k]\right|^2. \quad (58)$$

Note that $\beta_{\text{th}_{\text{DF/FDX,SI}}}[k] = 1$ (single transmission from S) when $F \to \infty$, which means that the SI $\to \infty$.

By contrast, if perfect SI cancellation is assumed (SI $\to 0$), $\beta_{\text{th}_{\text{DF/FDX}}}[k]$ is formulated as

$$\beta_{\text{th}_{\text{DF/FDX,nSI}}}[k] = \left(1 + \frac{\eta_{\text{pd,R}}^2 \left|H_{\text{fs}}^{\text{SR}}[k]\right|^2}{\eta_{\text{pd,D}}^2 \left|H_{\text{fs}}^{\text{RD}}[k]\right|^2}\right)^{-1}. \quad (59)$$

As indicated before, note that if the LoS path between S and D exists, single transmission is the best choice ($\beta_{\text{opt}_{\text{DF/FDX}}}[k] = 1$). If not, the power allocation has to be relied upon boosting either the S→R or the R→D path.
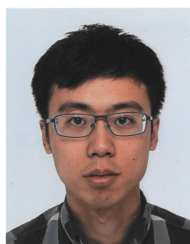
REFERENCES

[1] L. Hanzo, H. Haas, S. Imre, D. O'Brien, M. Rupp, and L. Gyongyosi, "Wireless myths, realities, and futures: from 3G/4G to optical and quantum wireless," Proc. IEEE, vol. 100, no. Special Centennial Issue, pp. 1853–1888, May 2012.

[2] X. Li, R. Zhang, and L. Hanzo, "Cooperative load balancing in hybrid visible light communications and WiFi," IEEE Trans. Commun., vol. 63, no. 4, pp. 1319–1329, Apr. 2015.

[3] C. Wang, F. Haider, X. Gao, X. You, Y. Yang, D. Yuan, H. M. Aggoune, H. Haas, S. Fletcher, and E. Hepsaydir, "Cellular architecture and key technologies for 5G wireless communication networks," IEEE Commun. Mag., vol. 52, no. 2, pp. 122–130, Feb. 2014.

[4] (2019) Status of IEEE 802.11 Light Communication TG. [Online]. Available: http://www.ieee802.org/11/Reports/tgbb_update.htm

[5] Z. Wang, Q. Wang, W. Huang, and Z. Xu, Visible Light Communications: Modulation and Signal Processing. Wiley-IEEE Press, 2018.

[6] B. G. Guzmán, V. P. G. Jiménez, M. C. Aguayo-Torres, H. Haas, and L. Hanzo, "Downlink performance of optical OFDM in outdoor visible light communication," IEEE Access, vol. 6, pp. 76 854–76 866, Nov. 2018.

[7] H. Haas, L. Yin, Y. Wang, and C. Chen, "What is LiFi?" J. Lightw. Technol., vol. 34, no. 6, pp. 1533–1544, Mar. 2016.

[8] C. Chen, D. Tsonev, and H. Haas, "Joint transmission in indoor visible light communication downlink cellular networks," in 2013 IEEE Globecom Workshops, Dec. 2013, pp. 1127–1132.

[9] I. Stefan, H. Burchardt, and H. Haas, "Area spectral efficiency performance comparison between VLC and RF femtocell networks," in 2013 IEEE International Conference on Communications (ICC), June 2013, pp. 3825–3829.

[10] C. Chen, S. Videv, D. Tsonev, and H. Haas, "Fractional frequency reuse in DCO-OFDM-based optical attocell networks," J. Lightw. Technol., vol. 33, no. 19, pp. 3986–4000, Oct. 2015.

[11] Z. Chen, D. A. Basnayaka, and H. Haas, "Space division multiple access for optical attocell network using angle diversity transmitters," J. Lightw. Technol., vol. 35, no. 11, pp. 2118–2131, June 2017.

[12] L. Zeng, D. C. O'Brien, H. L. Minh, G. E. Faulkner, K. Lee, D. Jung, Y. Oh, and E. T. Won, "High data rate multiple input multiple output (MIMO) optical wireless communications using white LED lighting," IEEE J. Sel. Areas Commun., vol. 27, no. 9, pp. 1654–1662, Dec. 2009.

[13] A. H. Azhar, T. A. Tran, and D. O'Brien, "A Gigabit/s indoor wireless transmission using MIMO-OFDM visible-light communications," IEEE Photon. Technol. Lett., vol. 25, no. 2, pp. 171–174, Jan. 2013.

[14] B. G. Guzmán, A. L. Serrano, and V. P. G. Jiménez, "Cooperative optical wireless transmission for improving performance in indoor scenarios for visible light communications," IEEE Trans. Consum. Electron., vol. 61, no. 4, pp. 393–401, Nov. 2015.

[15] B. G. Guzmán, A. A. Dowhuszko, V. P. G. Jiménez, and A. I. Pérez-Neira, "Robust cooperative multicarrier transmission scheme for optical wireless cellular networks," IEEE Photon. Technol. Lett., vol. 30, no. 2, pp. 197–200, Jan. 2018.

[16] O. Somekh, O. Simeone, Y. Bar-ness, A. M. Haimovich, U. Spagnolini, and S. Shamai, An Information Theoretic View of Distributed Antenna Processing in Cellular Systems. Auerbach Publication, CRC Press, 2007.

[17] O. Tipmongkolsilp, S. Zaghloul, and A. Jukan, "The evolution of cellular backhaul technologies: Current issues and future trends," IEEE Commun. Surveys Tuts., vol. 13, no. 1, pp. 97–113, First 2011.

[18] ETSI TS 136 300 V13.2.0, "Evolved universal terrestrial radio access (E-UTRA) and evolved universal terrestrial radio access network (E-UTRAN)," 2016.

[19] M. Rahnema, "Overview of the GSM system and protocol architecture," IEEE Commun. Mag., vol. 31, no. 4, pp. 92–100, Apr. 1993.

[20] J. Song, W. Ding, F. Yang, H. Yang, B. Yu, and H. Zhang, "An indoor broadband broadcasting system based on PLC and VLC," IEEE Trans. Broadcast., vol. 61, no. 2, pp. 299–308, June 2015.

[21] F. Delgado, I. Quintana, J. Rufo, J. A. Rabadan, C. Quintana, and R. Perez-Jimenez, "Design and implementation of an Ethernet-VLC interface for broadcast transmissions," IEEE Commun. Lett., vol. 14, no. 12, pp. 1089–1091, Dec. 2010.

[22] Y. Wang, N. Chi, Y. Wang, L. Tao, and J. Shi, "Network architecture of a high-speed visible light communication local area network," IEEE Photon. Technol. Lett., vol. 27, no. 2, pp. 197–200, Jan. 2015.

[23] H. Kazemi, M. Safari, and H. Haas, "A wireless optical backhaul solution for optical attocell networks," IEEE Trans. Wireless Commun., vol. 18, no. 2, pp. 807–823, Feb. 2019.

[24] J. Zhao, T. Q. S. Quek, and Z. Lei, "Heterogeneous cellular networks using wireless backhaul: Fast admission control and large system analysis," IEEE J. Sel. Areas Commun., vol. 33, no. 10, pp. 2128–2143, Oct. 2015.

[25] Y. Li, N. Pappas, V. Angelakis, M. Pióro, and D. Yuan, "Optimization of free space optical wireless network for cellular backhauling," IEEE J. Sel. Areas Commun., vol. 33, no. 9, pp. 1841–1854, Sept. 2015.

[26] O. Narmanlioglu, R. C. Kizilirmak, F. Miramirkhani, and M. Uysal, "Cooperative visible light communications with full-duplex relaying," IEEE Photon. J., vol. 9, no. 3, pp. 1–11, June 2017.

[27] Z. Na, Y. Wang, M. Xiong, X. Liu, and J. Xia, "Modeling and throughput analysis of an ADO-OFDM based relay-assisted VLC system for 5G networks," IEEE Access, vol. 6, pp. 17 586–17 594, 2018.

[28] R. C. Kizilirmak, O. Narmanlioglu, and M. Uysal, "Relay-assisted OFDM-based visible light communications," IEEE Trans. Commun., vol. 63, no. 10, pp. 3765–3778, Oct. 2015.

[29] C. Chen, D. A. Basnayaka, X. Wu, and H. Haas, "Efficient analytical calculation of non-line-of-sight channel impulse response in visible light communications," J. Lightw. Technol., vol. 36, no. 9, pp. 1666–1682, May 2018.

[30] F. Jin, X. Li, R. Zhang, C. Dong, and L. Hanzo, "Resource allocation under delay-guarantee constraints for visible-light communication," IEEE Access, vol. 4, pp. 7301–7312, 2016.

[31] H. L. Minh, D. O'Brien, G. Faulkner, L. Zeng, K. Lee, D. Jung, Y. Oh, and E. T. Won, "100-Mb/s NRZ visible light communications using a postequalized white LED," IEEE Photon. Technol. Lett., vol. 21, no. 15, pp. 1063–1065, Aug. 2009.

[32] C. Chen, D. A. Basnayaka, and H. Haas, "Downlink performance of optical attocell networks," J. Lightw. Technol., vol. 34, no. 1, pp. 137–156, Jan. 2016.

[33] H. Elgala, R. Mesleh, H. Haas, and B. Pricope, "OFDM visible light wireless communication based on white LEDs," in 2007 IEEE 65th Vehicular Technology Conference, Apr. 2007, pp. 2185–2189.

[34] L. Wang and L. Hanzo, "Dispensing with channel estimation: Differentially modulated cooperative wireless communications," IEEE Commun. Surveys Tuts., vol. 14, no. 3, pp. 836–857, Third 2012.

[35] B. Rankov and A. Wittneben, "Spectral efficient protocols for half-duplex fading relay channels," IEEE J. Sel. Areas Commun., vol. 25, no. 2, pp. 379–389, Feb. 2007.

[36] Z. Zhang, K. Long, A. V. Vasilakos, and L. Hanzo, "Full-duplex wireless communications: Challenges, solutions, and future research directions," Proc. IEEE, vol. 104, no. 7, pp. 1369–1409, July 2016.

[37] D. G. Brennan, "Linear diversity combining techniques," Proceedings of the IRE, vol. 47, no. 6, pp. 1075–1102, June 1959.

[38] A. Goldsmith, Wireless Communications. New York, NY, USA: Cambridge University Press, 2005.

[39] T. Wang, A. Cano, G. B. Giannakis, and J. N. Laneman, "High-performance cooperative demodulation with decode-and-forward relays," IEEE Trans. Commun., vol. 55, no. 7, pp. 1427–1438, July 2007.

[40] Y. Liu, X. Xia, and H. Zhang, "Distributed space-time coding for full-duplex asynchronous cooperative communications," IEEE Trans. Wireless Commun., vol. 11, no. 7, pp. 2680–2688, July 2012.

[41] J. Han, J. Baek, S. Jeon, and J. Seo, "Cooperative networks with amplify-and-forward multiple-full-duplex relays," IEEE Trans. Wireless Commun., vol. 13, no. 4, pp. 2137–2149, Apr. 2014.

[42] Q. Chen and X. Rui, "On the performance of full-duplex relaying under fading loop interference channel," in IET International Conference on Information Science and Control Engineering 2012, Dec. 2012, pp. 1–4.

[43] C. Zhong and Z. Zhang, "Non-orthogonal multiple access with cooperative full-duplex relaying," IEEE Commun. Lett., vol. 20, no. 12, pp. 2478–2481, Dec. 2016.

[44] A. E. Gamal and Y.-H. Kim, Network Information Theory. USA: Cambridge University Press, 2012.

[45] R. Jain, D. Chiu, and W. Hawe, "A quantitative measure of fairness and discrimination for resource allocation in shared computer system," DEC Technical Report 301, 1984.

[46] C. Chen and H. Haas, "Performance evaluation of downlink cooperative multipoint joint transmission in lifi systems," in Proc. IEEE Globecom Workshops, Dec. 2017, pp. 1–6.

[47] J. Vucic, C. Kottke, S. Nerreter, K. Langer, and J. W. Walewski, "513 Mbit/s visible light communications link based on DMT-modulation of a white LED," J. Lightw. Technol., vol. 28, no. 24, pp. 3512–3518, Dec. 2010.

[48] K. Dong, X. Liao, and S. Zhu, "Link blockage analysis for indoor 60GHz radio systems," Electron. Lett., vol. 48, no. 23, pp. 1506–1508, Nov. 2012.

[49] BS 8300-1:2018/BS 8300-2:2018, "Design of an accessible and inclusive built environment. Buildings/External environment. Code of practice," 2018.

[50] J. L. Taylor, "Reflectance measurements of materials used in the solar industry," Technical Note, UV/Vis/NIR, 2009.

[51] S. Webster, "Designing an LTE network using EDX SignalPro," EDX Wireless, Technology White Paper, Sept. 2010.

VÍCTOR P. GIL JIMÉNEZ (S'00–AM'02–M'03–SM'12) received the B.S and the M.S in Telecommunication degree in 1998 and 2001, from the University of Alcalá and University Carlos III of Madrid, respectively, and the Ph.D. degree in 2005 from the University Carlos III of Madrid, all of them with honours. He is with the department of Signal Theory and Communications at the University Carlos III of Madrid as Associate Professor. He worked at the Spanish Antarctica Base in 1999 as Communications Staff. He visited University of Leeds (UK), Chalmers Technical University (Sweden) and Instituto de TelecomunicaĀğoes (Portugal) in 2003, 2004 and 2008 - 2010, respectively. He has also led several private and national Spanish projects and has participated in several European and international projects. He holds one patent. He has received the Master Thesis and a Ph.D. Thesis Award by the Professional Association of Telecommunication Engineers of Spain in 1998 and 2006, respectively. He has published over 50 journal/conference papers and 5 book chapters. His interests are in the field of the advanced multicarrier systems for wireless radio and visible light communications. He held the IEEE Spanish Communications and Signal Processing Joint Chapter chair (2015 - 2019).

BORJA GENOVÉS GUZMÁN (S'14) received his B.Sc. from the University Carlos III of Madrid in 2013, and a double M.Sc. degree in electrical engineering from the University Carlos III of Madrid and the Institut Mines-Télécom (France) in 2015, both with honours. He received the First prize in Graduation National Awards by the Ministry of Education, Culture and Sports of Spain. He received the Ph.D. degree from the University Carlos III of Madrid in 2019. He was a visiting scholar in the Southampton Wireless Group at The University of Southampton and in the LiFi Research and Development Centre at The University of Edinburgh, in 2017 and 2018, respectively. He was a recipient of an FPU scholarship from the Spanish Ministry of Education, Culture and Sports of Spain. He has participated in several national and European projects. He is currently a post-doc researcher at IMDEA Networks Institute. His current research focuses on new techniques to improve the efficiency of optical wireless communications systems, next generation wireless networks and mobile communications.

HARALD HAAS (S'98–AM'00–M'03–SM'16–F'17) FREng FRSE FIEEE FIET is a full Professor at the University of Edinburgh. He is a co-founder of pureLiFi Ltd. He is also the Director of the LiFi Research and Development Center (LRDC) at the University of Edinburgh. His research interests are in optical wireless communications and spatial modulation.

Professor Haas holds 47 patents and has more than 30 pending patent applications. He has published more than 500 conference and journal papers including a paper in Science. He has been on the Thomson Reuters list of highly cited Scientists in 2017, 2018 and 2019. Prof Haas has delivered 50 invited keynotes talks at international conferences and workshops. He delivered two TED Global talks which together have been watched online more than 5 million times. He is co-recipient of several best paper awards at IEEE conferences such as ICC, VTC, WCNC and PIMRC.

In 2012, he was the recipient of the prestigious Established Career Fellowship from the EPSRC. In 2014, he was selected by EPSRC as one of ten RISE (Recognising Inspirational Scientists and Engineers) Leaders in the UK. In 2016, he received the outstanding achievement award from the International Solid State Lighting Alliance. In 2017 he received a Royal Society Wolfson Research Merit Award. In 2018 he received a three-year EPSRC Established Career Fellowship extension. He is recipient of the James Evans Avant Garde Award in 2019 awarded by the IEEE Vehicular Technology Society.

CHENG CHEN received the B.Eng. degree in electronic and electrical engineering from the University of Strathclyde, Glasgow, U.K., in 2011, the M.Sc. degree in communications and signal processing from the Imperial College, London, U.K., in 2012, and the Ph.D. degree in electrical engineering from the University of Edinburgh, Edinburgh, U.K., in 2017. He is currently employed as a Research Associate with the Li-Fi Research and Development Centre, the University of Edinburgh and is working in the field of visible light communications.
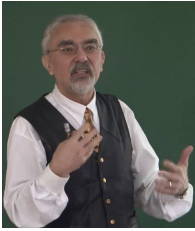
B. Genovés Guzmán *et al.*: Reflection-based Relaying Techniques in Visible Light Communications: Will It Work?

IEEE *Access*

LAJOS HANZO (M'91–SM'92–F'04)
Lajos Hanzo http:www-mobile.ecs.soton.ac.uk, https:en.wikipedia.orgwikiLajos_Hanzo FREng, FIEEE, FIET, Fellow of EURASIP, DSc has received his Master degree and Doctorate in 1976 and 1983, respectively from the Technical University (TU) of Budapest. He was also awarded Honorary Doctorates by the TU of Budapest (2009) and by the University of Edinburgh (2015). He is a Foreign Member of the Hungarian Academy of Sciences and a former Editor-in-Chief of the IEEE Press. He has served as Governor of both IEEE ComSoc and of VTS. He has published 1900+ contributions at IEEE Xplore, 19 Wiley-IEEE Press books and has helped the fast-track career of 119 PhD students. Over 40 of them are Professors at various stages of their careers in academia and many of them are leading scientists in the wireless industry.

• • •